Polish Society of Composite Materials
Polskie Towarzystwo Materiałów Kompozytowych

21: 1-2 (2021) 12-21

COMPOSITES THEORY AND PRACTICE
ISSN: 2084-6096
ISSN (online): 2299-128X

Shahinoor Alam*, Mohammad Asaduzzaman Chowdhury

Dhaka University of Engineering and Technology, Department of Mechanical Engineering, Gazipur-1707, Bangladesh
**Corresponding author. E-mail: majshahin4282@gmail.com*

Received (Otrzymano) 17.07.2020

THERMAL GRAVIMETRIC ANALYSIS OF GLASS FIBER REINFORCED COMPOSITE FOR UNDERSTANDING THE IMPACT OF COPPER OXIDE IN RELATION TO TITANIUM OXIDE FILLER PARTICLES

In this work, the composite samples required to investigate their thermal properties were fabricated employing the conventional hand lay-up technique, followed by a light compression molding process. A fixed weight of plain woven glass fiber and epoxy with four different types of fillers as calcium carbonate ($CaCO_3$), aluminum oxide (Al_2O_3), magnesium oxide (MgO) and titanium oxide (TiO_2) or copper oxide (CuO) of different weights (5, 10 and 15 g) were studied. According to thermal gravimetric analysis (TGA), it was observed that the melting point (T_m) and glass-transition temperature (T_g) are affected by the presence of CuO and TiO_2, which indicate the degree of composite crystallinity established by the stronger interfacial interaction by the CuO than that of the TiO_2 particles and the amorphous region of the chain. These studies were supported by examination of the surface morphology of the composites by means of scanning electron microscopy (SEM).

Keywords: composite, glass fiber, epoxy, thermal characteristics, TGA, $CaCO_3$, Al_2O_3, MgO, TiO_2, CuO

INTRODUCTION

Because of their adaptable and widespread use, flexibility in design, enhanced thermal characteristics and desired mechanical properties compared with simple alloys, composites have already attained a strong position in modern industries. Tremendous work has been done on thermosetting polymers [1-4] and their composites [5-7] over the decades. Epoxy resins are some of the most frequently used polymer matrices in glass fiber composites due to their versatile applications in the engineering field [8-10]. Composites fabricated with epoxy as the base material can possibly replace conventional metal designs. The modification of current polymer composites is one of the approaches to develop new polymer composites to be used for intended applications. In most engineering applications, functional fillers are used in fiber reinforced polymer matrix composites (PMCs) to draw attention to the development of advanced PMCs as well as hybrid PMCs, which are presently going through huge innovative research [11].

Many researchers have studied the influencing factors of composites, the characteristics of composites [12-14] and several modifications have been made to improve the thermal stability of the material. In composite production, it is absolutely essential to measure the thermal stability of the material to ascertain the range of temperature in which it can be used without degradation. Thermoplastics are used to increase the toughness of thermosetting resins for their high glass transition temperature [15-17]. Thermogravimetric analysis (TGA) is an important thermal analysis technique, which has wide applications in characterizing polymer materials [18]. Through thermal analysis, the properties of polymeric materials are ascertained as a function of temperature.

The principal potential benefits of exploiting modified composites containing a similar nature of fiber are to change the thermal, mechanical and physical properties to suit the end use application. Hence, it is obvious to modify the polymer matrix to use it for the intended purposes. A popular method to modify the properties of the base materials is to add fillers to the polymer matrix [19]. The modification of epoxy resins by the addition of filler materials reduces the cost and improves the mechanical, thermal and electrical properties of the resins significantly [20]. Various filler materials are introduced into fiber reinforced polymer composites (FRPCs) to develop the stiffness and heat deflection, reduce shrinkage and voids and to give composites a more solid appearance. Research is continuing in fillers incorporated into FRPCs to obtain high mechanical and wear resistance properties to employ these ma-

terials in various mechanical parts, for example, chute liners, brake pads, clutches and gears [21]. Glass fiber composites modified with $CaCO_3$, Al_2O_3 and TiO_2 have numerous applications in different industrial sectors and leading technologies like armor, ballistics, helicopter blades, air turbine blades, pneumatic reinforcement and sporting goods [22-24]. Against this background, the objective of this work is to investigate the thermal characteristics of glass fiber reinforced composites by analyzing the impact of CuO in relation to TiO_2 when modified with $CaCO_3$, Al_2O_3, MgO and TiO_2 or CuO in two different instances.

EXPERIMENTAL PART

Fabrication and investigation of composites

Six types of epoxy-based fiber reinforced plastic (FRP) composites containing various fillers were produced using the hand lay-up method (Fig. 1a). Various percentages (weight related) of resin, epoxy hardener, fillers, and fibers were used in the experiments, as presented in Tables 1 and 2. To obtain the ideal degree of homogeneity, all the composite samples were laid up similarly and comparable light pressure was applied in each cases.

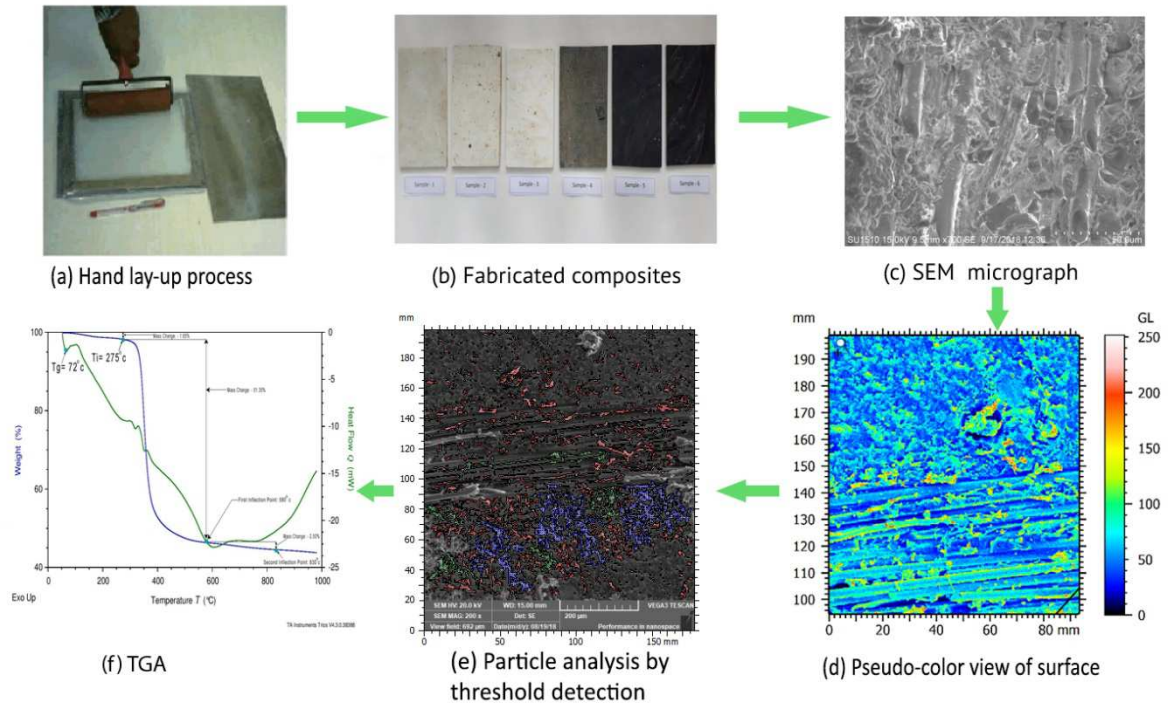

Fig. 1. Fabrication and investigation of sample composites

TABLE 1. **Composition of FRP for experiment – 1 (by weight)**

Composite sample	Fiber stacking sequence	Compositions							
		Matrices Wt [g]		Reinforcement Wt [g]					
		Epoxy (LY556)	Araldite (HY951)	Glass fiber	Fillers				
					$CaCO_3$	Al_2O_3	MgO	TiO_2	Total
S1	G/ G/ G/ G/ G	150	15	265	5	5	5	5	20
S2	G/ G/ G/ G/ G	150	15	265	10	10	10	10	40
S3	G/ G/ G/ G/ G	150	15	265	15	15	15	15	60

TABLE 2. **Composition of FRP for experiment – 2 (by weight)**

Composite sample	Fiber stacking sequence	Compositions							
		Matrices Wt [g]		Reinforcement Wt [g]					
		Epoxy (LY556)	Araldite (HY951)	Glass fiber	Fillers				
					$CaCO_3$	Al_2O_3	MgO	CuO	Total
S4	G/ G/ G/ G/ G	150	15	265	5	5	5	5	20
S5	G/ G/ G/ G/ G	150	15	265	10	10	10	10	40
S6	G/ G/ G/ G/ G	150	15	265	15	15	15	15	60

Analyzing techniques

Thermal investigation

Thermal gravimetric analysis (TGA) was carried out somewhere in the range of 50 and 1000°C in liquid nitrogen, with the heating rate of 5°C min^{-1} by means of a TGA Instrument (SDT650 Serial No 0650-0180) as shown in Figure 2. Thereafter, the specimens for differential scanning calorimetric (DSC) and thermogravimetric (TG) analysis were acquired from the fabricated samples to measure the heat deflection temperature (HDT) by cutting perpendicular to the glass mat. Specimens weighing 25-45 mg were employed for each round of TG analysis.

Fig. 2. TGA of prepared composite

The information collected from the thermal response was compiled in a plot with either the underlying mass percentage or the quantity of heat along the y-axis when correlated with the temperature along the x-axis. The previously mentioned plot is called a TGA graph, which showed a gradual downward slope. It is possible to plot the first order of the TGA graph (DTG graph) to determine the inflection points that are useful for differential thermal investigation and the required correlations.

Imaging technique

The microstructure of the composites was examined by means of a Hitachi SU-1510 scanning electron microscope (SEM), as seen in Figure 3. The specimens were prepared for SEM examination according to ASTM standard D 5299.

The composite specimens presented in Figure 3a were properly cleaned, air-dried and prepared for SEM observation. Thereafter, a thin and small sized platinum film was evaporated on the above composite specimens so as to augment the conductivity before taking the micrographs. Figure 3b shows the SEM set up and analysis.

RESULTS AND DISCUSSION

Thermal investigation

The plotting of the TGA is performed based on the change in temperature happening inside the substance, which is developed by applied changes or internal reactions. Usually, the specimen loads are sensitive to an ascent in temperature. This resultant graph is known as a thermogram and provides the basic data concerning the underlying thermal structure/stability of the specimen, as well as the soundness, structure of the fabricated samples and the composition of the components. Usually every material has a separate composition as well as a separate thermogram that helps in its recycling process.

The plotting of the weight loss against time or temperature (termed as a TGA graph) and heat flow versus temperature (known as a DSC graph) are the ultimate consequences of TGA investigation as demonstrated in Figures 4 to 9. There are two temperatures notable in the TGA graph (Fig. 4): the start of the decomposition temperature (T_i = 275°C) and the final temperature (T_f = not seen), which indicates the most minimal conceivable temperature wherein weight loss starts to become visible, as well as the least conceivable temperature wherein its decomposition is completed. The stretch and reaction temperatures are firmly predicated on the conditions of the analyses. Therefore, they cannot have any fixed quantities. Melting (T_m) happens to crystalline polymer, whereas glass transition (T_g) happens exclusively to the polymer inside a nebulous condition. It is possible for the crystalline polymer of a composite sample to contain and display both the temperatures of glass transition and melting point. Nevertheless, the melting chain and amorphous areas of the composites may not experience the same.

a) Composite specimens for SEM (ASTM D5299) b) Scanning of composite

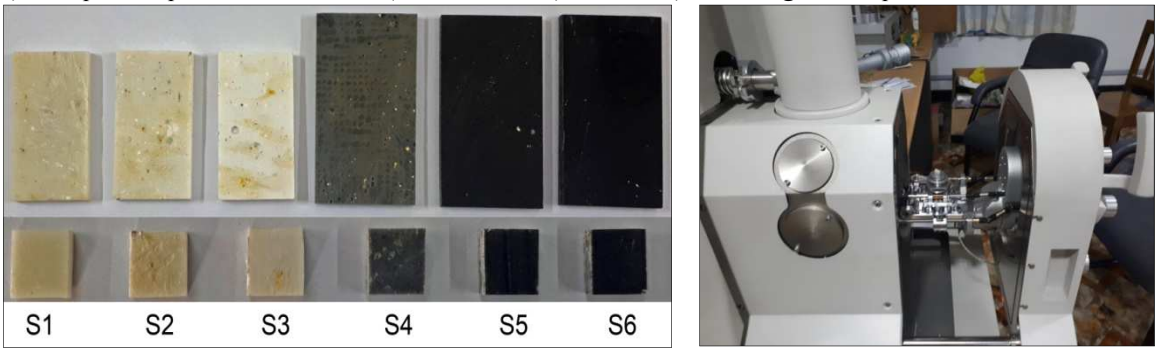

Fig. 3. Scanning of composites

The test composites (S1, S2 and S3) from investigation 1 with TiO_2 have glass transition temperatures (T_g) of 72, 74 and 72°C, respectively, as demonstrated in Figures 4-6. Then, test composites (S4, S5 and S6) from investigation 2 have glass transition temperatures of 75, 75 and 88°C, respectively, which are presented in Figures 7- 9.

(a) DSC Curve

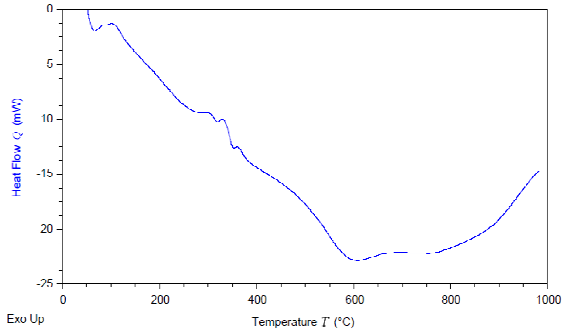

(b) TGA Curve

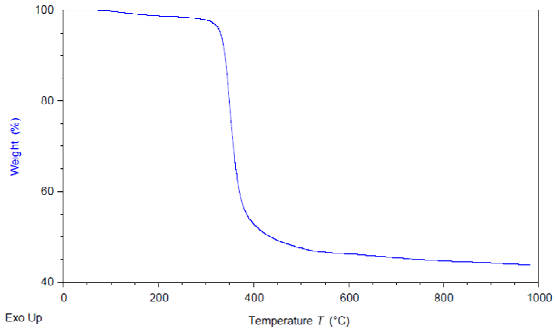

Fig. 4. Differential scanning calorimetric (DSC) and thermogravimetric analysis (TGA) of composite sample 1

(a) DSC Curve

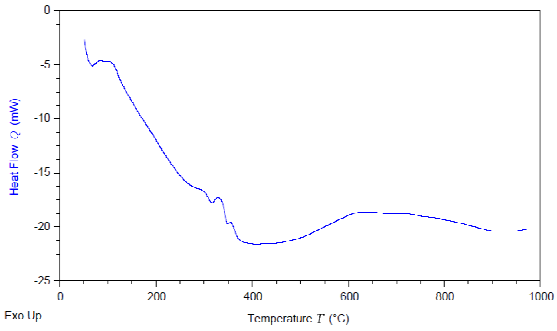

(b) TGA Curve

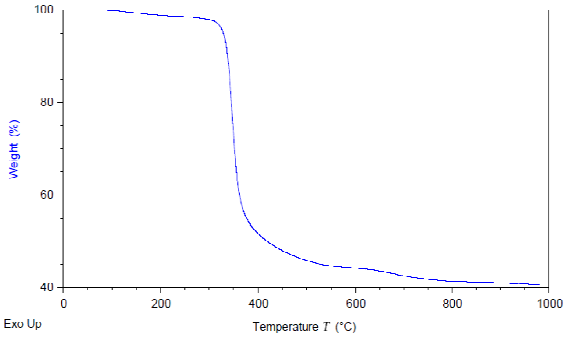

Fig. 5. Differential scanning calorimetric (DSC) and thermogravimetric analysis (TGA) of composite sample 2

(a) DSC Curve

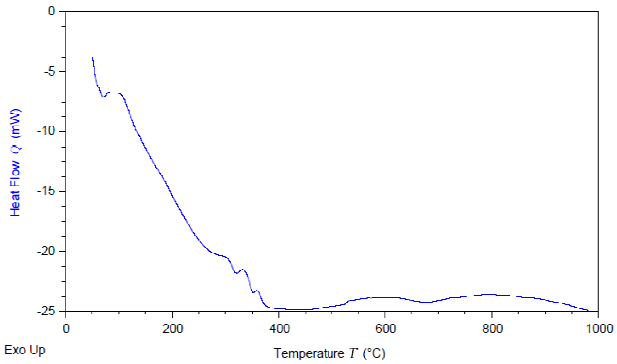

(b) TGA Curve

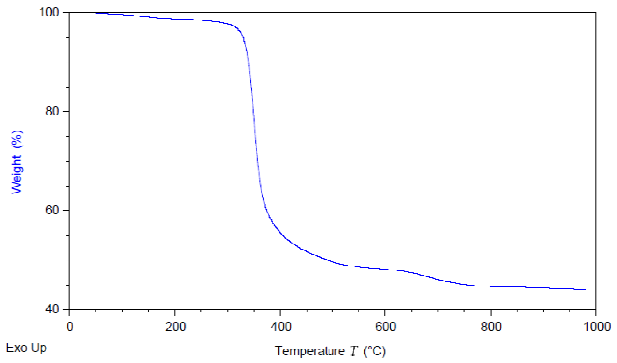

Fig. 6. Differential scanning calorimetric (DSC) and thermogravimetric analysis (TGA) of composite sample 3

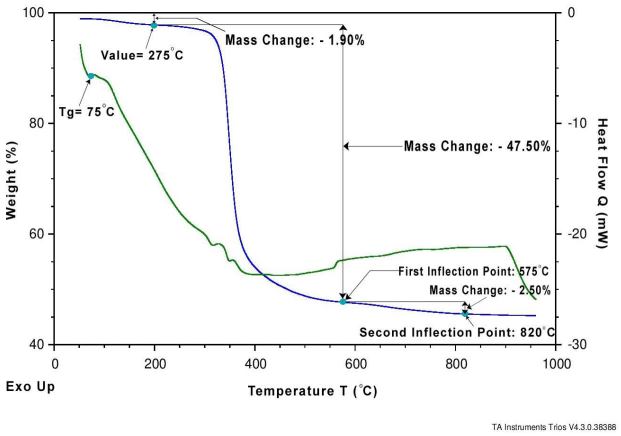

Fig. 7. Composite sample 4 DSC/TGA curves

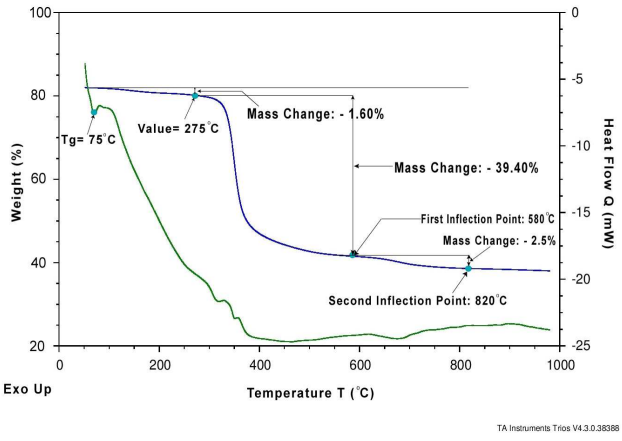

Fig. 8. Composite sample 5 DSC/TGA curves

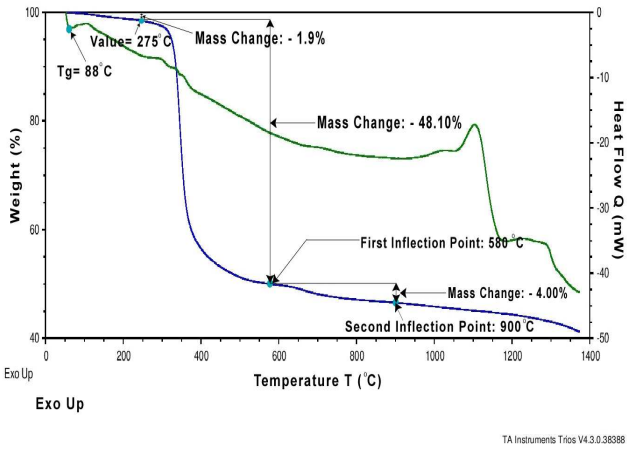

Fig. 9. Composite sample 6 DSC/TGA curves

The test composites fabricated with the TiO_2 filler material exhibit a lower glass transition temperature than that of the composites produced with the CuO filler material. This demonstrates the enhanced thermal and mechanical properties of the composites fabricated with CuO than of the composites produced with TiO_2.

Two factors were considered to take a decision on setting the ranges of temperature regarding the weight loss (decomposition) of the composites. Volatility is the first challenge – this includes water as well as residual solvents. As indicated by the temperature, a similar result was found across all the conducted tests (approximately 1-2%) at 275°C. The subsequent issue is the inflection point because all the previously mentioned tests were found to mirror a progressive adjustment of the gradient within the range of 580-590°C. The development of the primary curve was expected to precisely indicate the point of inflection. As shown in Table 3 and Figure 10, there are changes in the results among the specimens.

TABLE 3. **TGA results of prepared composites**

Sample	Glass transition temperature [°C]	Weight loss in percentage (50 to 275°C)	Weight loss in percentage (275°C to first inflection)	Initial/first inflection point [°C]	Second/ subsequent inflection point [°C]	Weight loss in percentage (from first to second inflection point)
S1	72	1.65	51.35	580	830	2.50
S2	74	1.80	54.20	590	840	3.25
S3	72	1.75	50.25	590	820	4.50
S4	75	1.90	47.50	575	820	2.50
S5	75	1.60	39.40	580	820	2.50
S6	88	1.90	48.10	580	900	4.00

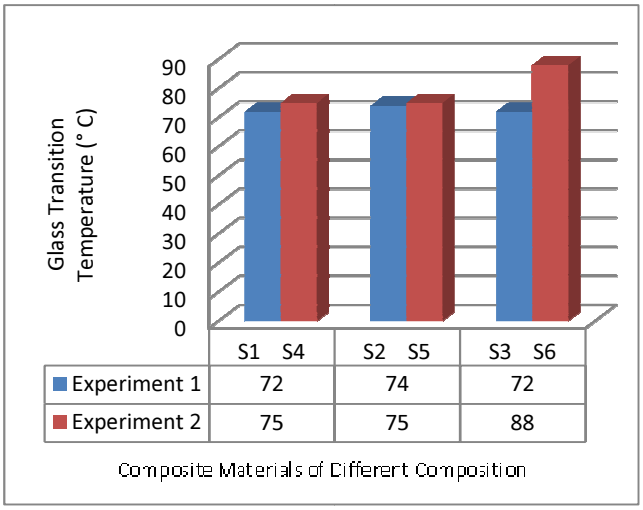

Fig. 10. Trends of glass transition temperature of composite samples

Micrograph analysis

SEM examination of the composites was performed to determine the morphology of the materials, verify uniform distribution of the filler materials and assess the continuity of the glass fibers. Many variations in the inner construction and the distribution of the filler materials of the fabricated composites were noticed. All the specimens (Fig. 11) showed consistency in the filler distribution and continuation of glass fiber all through them. Important changes in the microstructure of the materials fabricated with CuO were observed.

The SEM micrographs of the cross-sectional layer of the specimens are shown in Figure 11. From this Figure, it can be seen that the bonding between the matrix, fillers and fibers is stronger in the S4, S5 and S6 test specimens as compared with S1, S2 and S3. This is the reason why these samples show enhanced mechanical properties. Furthermore, specimen S2 (Fig. 11b) exhibits inadequate bonding and interfacial adhesion between the fibers, fillers and matrix of the specimen and also some voids were found in it, which ultimately degrade the thermal and mechanical properties of fabricated composite sample 2.

The microstructure of the cross-section of the glass fiber composite filled with CuO showed a smooth shape (when contrasted with the TiO_2 filler) and an internal construction free from voids as demonstrated in Figure 11c. The lack of adhesion between the glass fiber laminate and the filler materials is evident on the fractured surfaces. This is indicative of insufficient interaction at the interfacial level and potentially elucidates the decline in the quality of the thermal and mechanical properties, as depicted in Figure 11b. There is a positive relationship between the reinforcing fibers and functional fillers. Therefore, the above fact may clarify the reasons for the poor characteristics of the composite considering the fact that the stress transformation was less efficacious in that particular type of composite. In general, the two composites showed good adhesion at the interfacial level with CuO and TiO_2. However,

the composite that includes CuO displayed better stress distribution. Moreover, when the mean equivalent diameter and projected area of functional particles are increased, the interfacial adhesion and bonding of the particles with the fibers are improved (Figs. 11-13 and Table 4).

(a) Sample 1

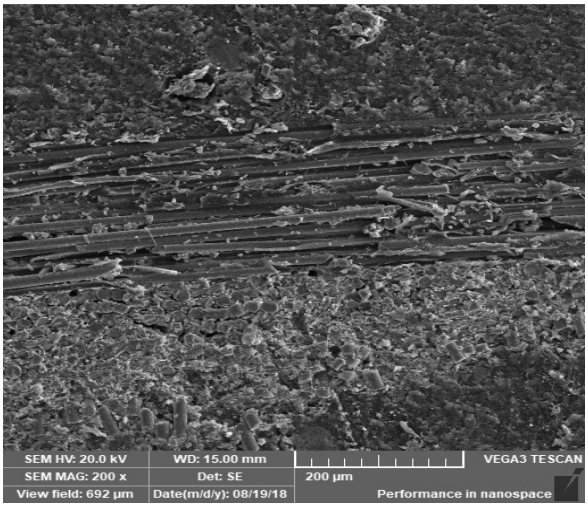

(b) Sample 2

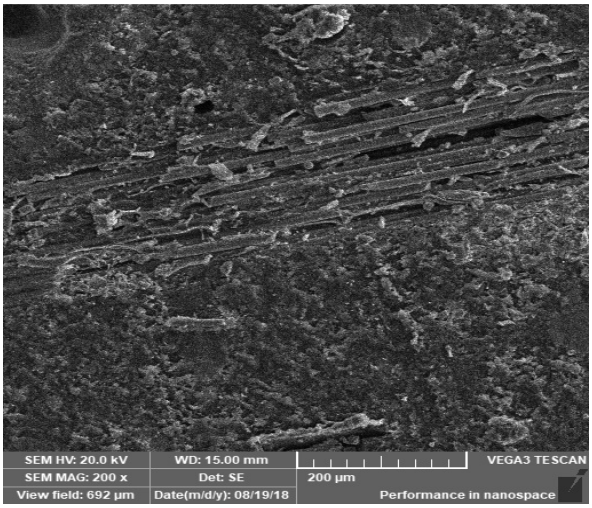

(c) Sample 3

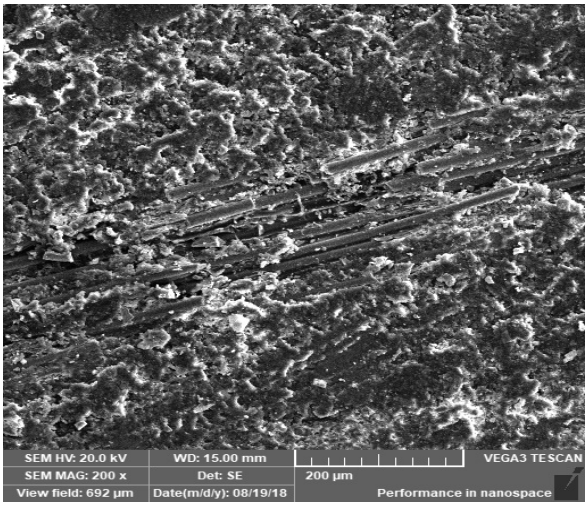

(d) Sample 4

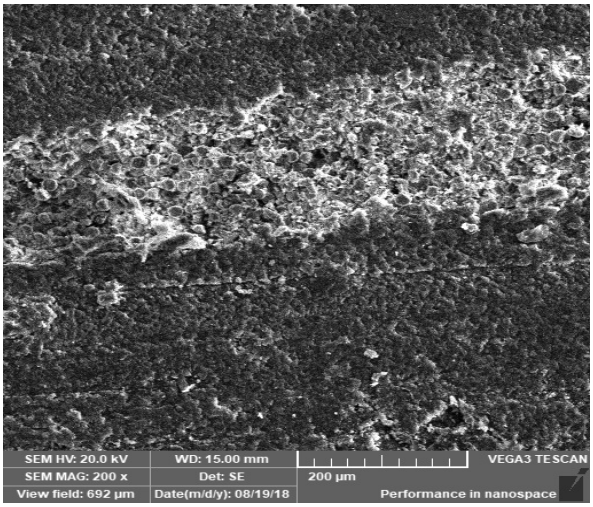

(e) Sample 5

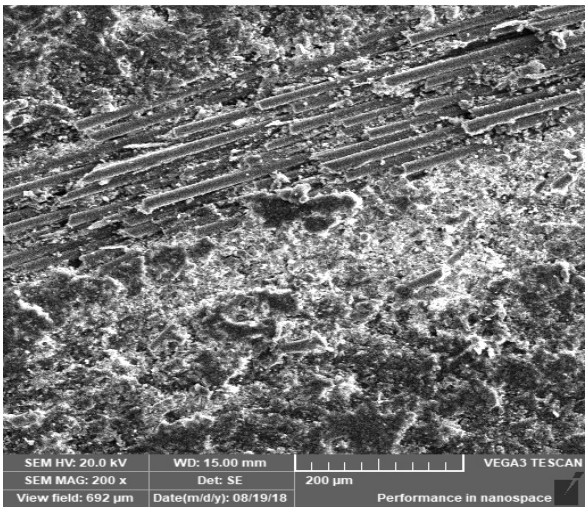

(f) Sample 6

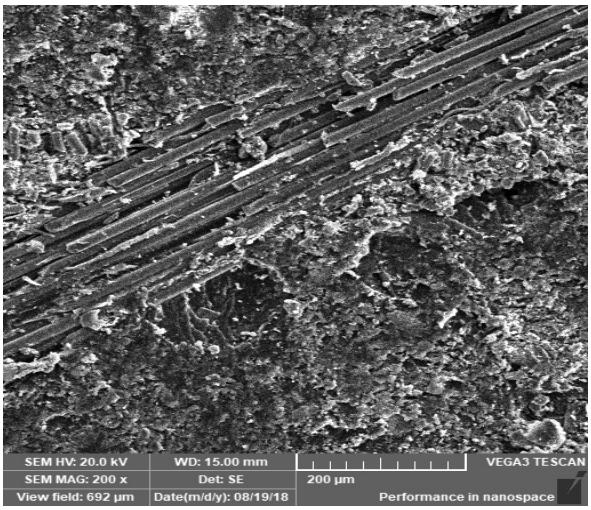

Fig. 11. Cross-sectional SEM micrographs of all composite samples

(a) Sample S1

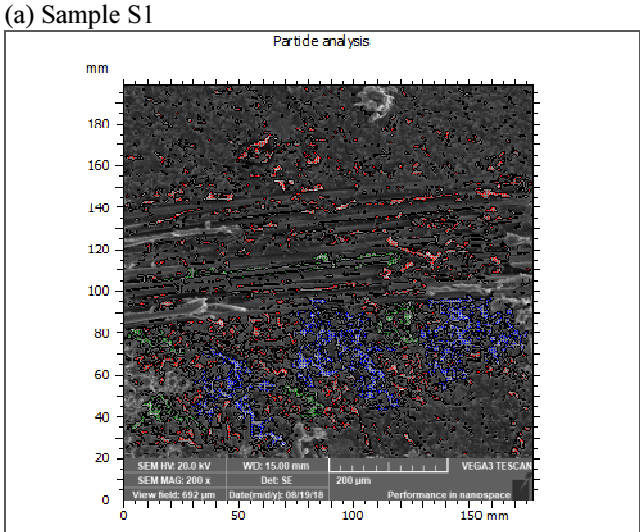

Information	
Method	Threshold detection
Number of particles	4440

Parameters	Default classification	Projected area	Equivalent diameter	Form factor
Unit		mm²	mm	
Particle #2624	C	735.3	30.60	0.0056 21
Particle #2587	C	694.4	29.78	0.0059 85
Particle #3130	C	462.9	24.28	0.0098 59
Particle #2179	B	229.5	17.09	0.01227
Particle #2652	B	153.4	13.97	0.0244
Particle #3702	B	140.6	13.38	0.0316
Mean	*****	1.519	0.7176	0.7673

(b) Sample S2

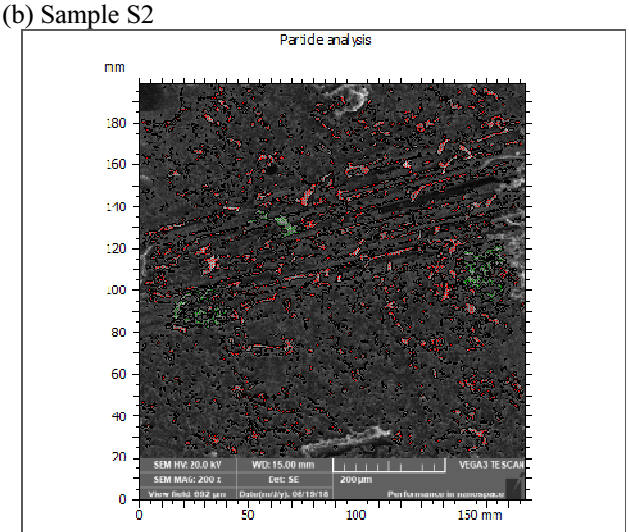

Information	
Method	Threshold detection
Number of particles	9595

Parameters	Default classification	Projected area	Equivalent diameter	Form factor
Unit		mm²	mm	
Particle #4254	B	239.0	16.51	0.01774
Particle #5226	B	156.3	14.55	0.01899
Particle #3256	B	94.98	11.00	0.04465
Particle #842	A	79.64	10.07	0.04846
Particle #5090	A	72.03	9.576	0.03531
Particle #4230	A	71.07	9.500	0.05401
Mean	*****	0.6075	0.5697	0.7803

(c) Sample S3

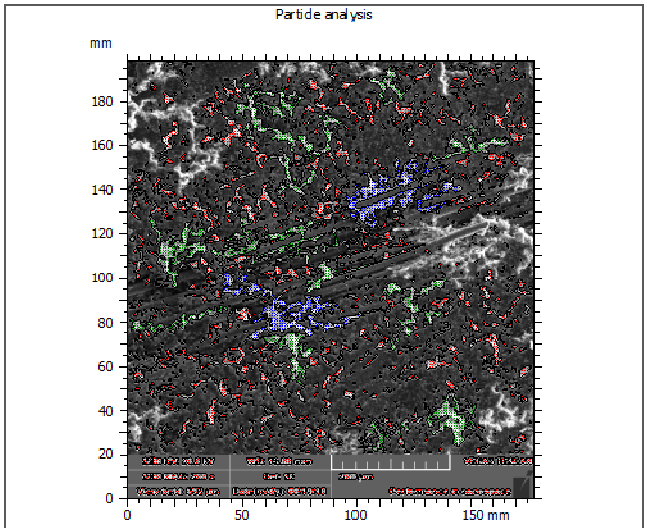

Information	
Method	Threshold detection
Number of particles	4622

Parameters	Default classification	Projected area	Equivalent diameter	Form factor
Unit		mm²	mm	
Particle #1152	C	467.6	24.40	0.01314
Particle #2460	C	460.2	24.21	0.01552
Particle #261	B	271.1	18.58	0.02479
Particle #1876	B	235.3	17.31	0.03266
Particle #3921	B	216.9	16.62	0.05028
Particle #2564	B	198.4	15.89	0.03283
Mean	*****	1.671	0.7484	0.7700

(d) Sample S4

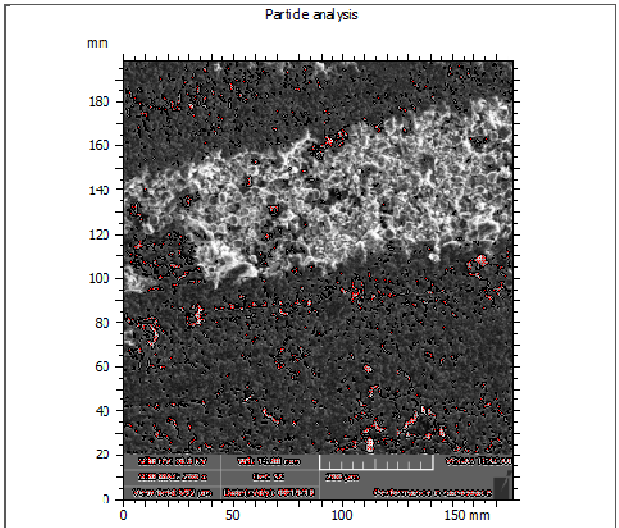

Information	
Method	Threshold detection
Number of particles	6398

Parameters	Default classification	Projected area	Equivalent diameter	Form factor
Unit		mm²	mm	
Particle #6487	A	53.24	8.234	0.18085
Particle #3820	A	52.13	8.147	0.16932
Particle #6491	A	45.32	7.646	0.19846
Particle #3559	A	41.20	7.242	0.1071
Particle #2735	A	35.32	6.763	0.1830
Particle #5662	A	32.34	6.417	0.1789
Mean	*****	0.5068	0.5485	0.7837

(e) Sample S5

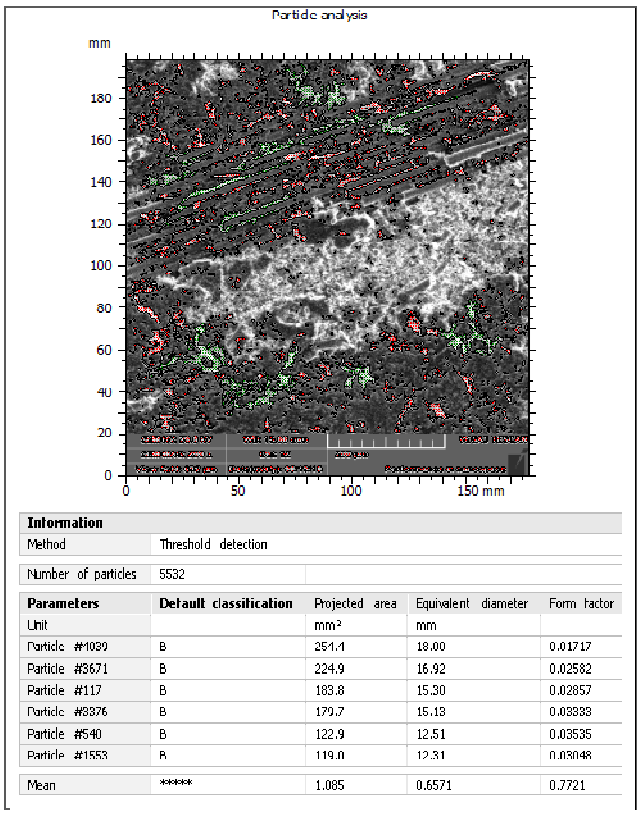

Information	
Method	Threshold detection
Number of particles	5532

Parameters	Default classification	Projected area	Equivalent diameter	Form factor
Unit		mm²	mm	
Particle #1039	B	254.4	18.00	0.01717
Particle #3671	B	224.9	16.92	0.02582
Particle #117	B	183.8	15.30	0.02857
Particle #3876	B	179.7	15.13	0.03838
Particle #540	B	122.9	12.51	0.03535
Particle #1553	B	119.0	12.31	0.03048
Mean	*****	1.085	0.6571	0.7721

(f) Sample S6

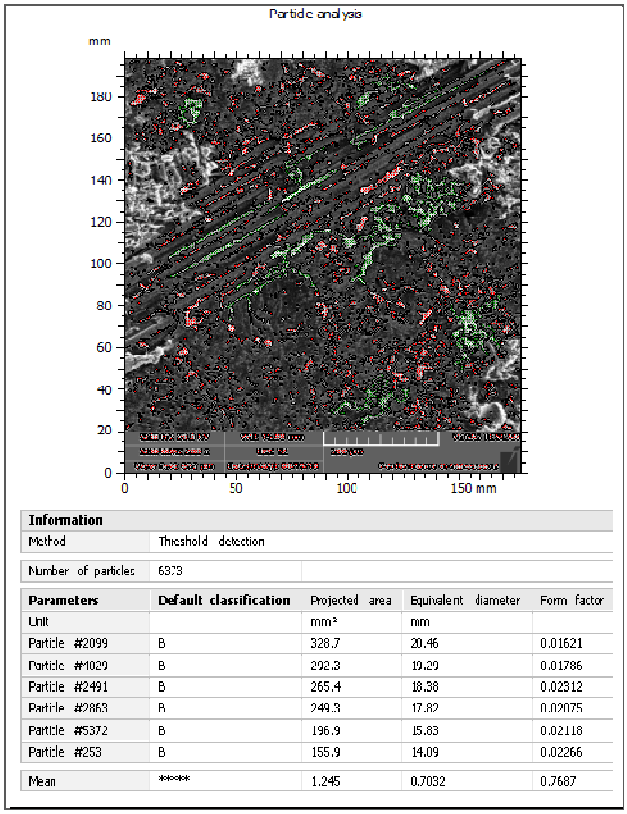

Information	
Method	Threshold detection
Number of particles	6878

Parameters	Default classification	Projected area	Equivalent diameter	Form factor
Unit		mm²	mm	
Particle #2099	B	328.7	20.46	0.01621
Particle #1029	B	292.3	19.29	0.01786
Particle #2491	B	265.4	18.38	0.02312
Particle #2863	B	249.3	17.82	0.02075
Particle #5372	B	196.9	15.63	0.02118
Particle #253	B	155.9	14.09	0.02266
Mean	*****	1.245	0.7032	0.7687

Fig. 12. Particle parameters using threshold detection method

(a) Sample S1

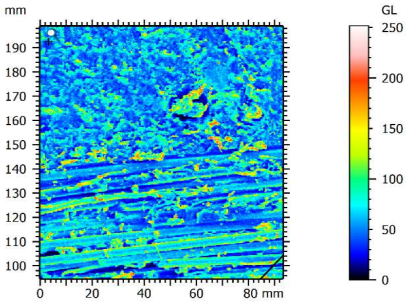

(b) Sample S2

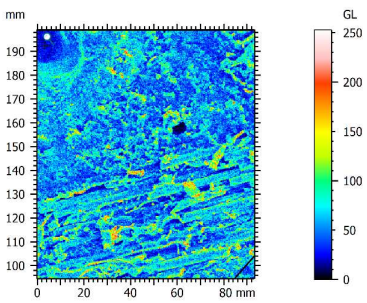

(c) Sample S3

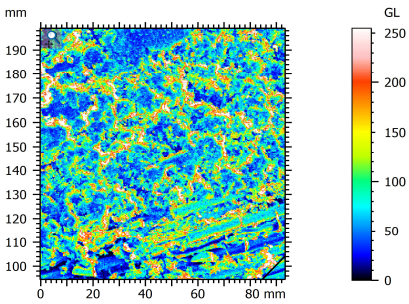

(d) Sample S4

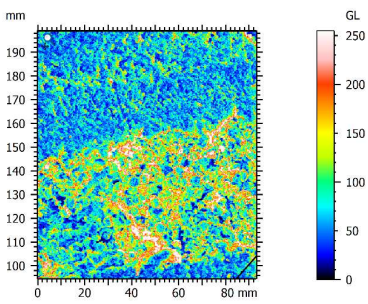

(e) Sample S5

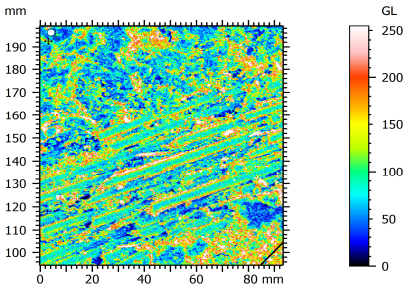

(f) Sample S6

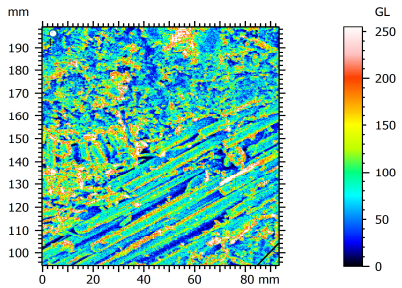

Fig. 13. Pseudo-color view of surface of composite samples

TABLE 4. **Particle parameters of composite samples using threshold detection method by default classification**

Composite sample	Mean projected area [mm^2]	Mean equivalent diameter [mm]	Mean form factor
S1	1.52	0.72	0.767
S2	0.61	0.55	0.780
S3	1.67	0.75	0.770
S4	0.51	0.55	0.784
S5	1.09	0.66	0.772
S6	1.25	0.70	0.769

Thermal surface morphology characterization

Figure 14a-c shows the change in the cross-sectional morphology of the sample S4 at different temperatures. It is observed from the figure that the embedded fibers distort significantly with the increase in temperature. The bonding strengths of the fibers with the resin deformed in an irregular manner due to the drastic change in the mechanical properties.

(a) Sample S4 at ambient temperature

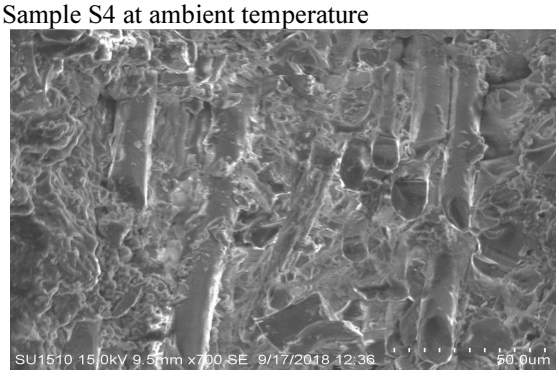

(b) Sample S4 at 40ºC

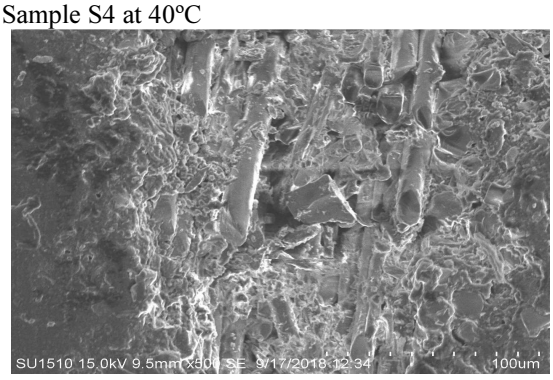

(c) Sample S4 at 60ºC

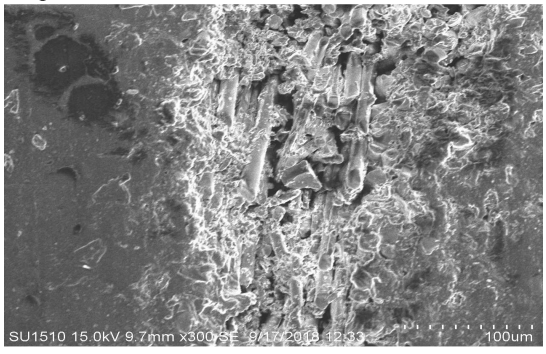

Fig. 14. Cross-sectional SEM micrographs of S4 sample at different temperatures

FTIR analysis was performed to ascertain the functional groups which may be responsible for the chemical reaction or elemental components or resin, hardener and fibers with the rise in temperature. The changes in the spectrum are indicated in Figure 15a, b.

(a) FTIR of Sample 1 at ambient temperature

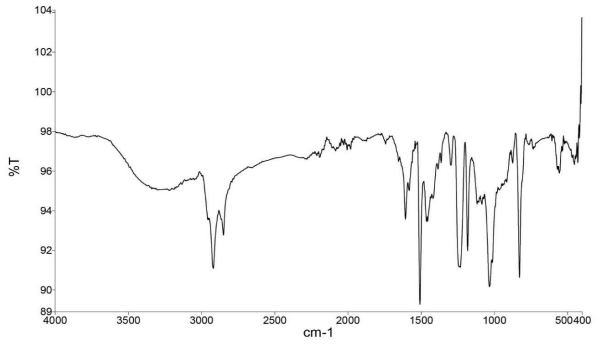

Sample Name	Description	Saved or unsaved State	Spectrum quality check summary
Composite sample 1	Sample 431 By Administrator. September 19, 2018	Saved	The quality checks indicate a weak band warning for the sample

(b) FTIR of Sample S1 at 60ºC

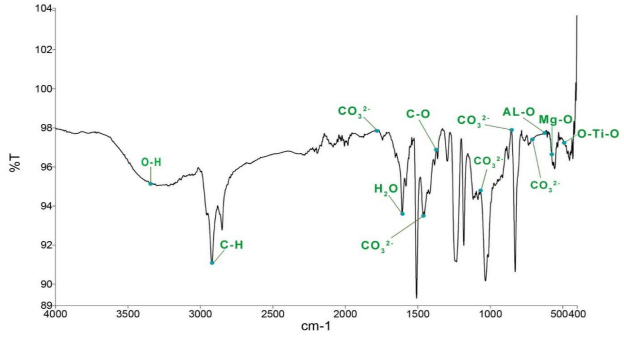

Sample Name	Description	Saved or unsaved State	Spectrum quality check summary
Composite sample 1	Sample 431 By Administrator. September 19, 2018	Saved	The quality checks indicate a weak band warning for the sample

Fig. 15. Change in nature of FTIR spectrum at different temperatures

CONCLUSIONS

In the commercial industry, the use of filler materials for polymers is a typical practice. This helps to enhance the stiffness, toughness, hardness, thermal stability, and mold shrinkage, as well as minimizes the production costs to a great extent. Different fillers were used to fabricate glass fiber composites to observe how they affect the interfacial adhesion behavior of the fiber with the matrix as well as the thermal stability of the

composites. The agglomeration of the micro filler materials in the composite matrix was examined in the micrographs of the composite samples, which revealed the microstructural details of the underlying cracked surfaces of the composites. The SEM examination also demonstrated that the light compression molding technique is suitable to decrease the number voids in the composites. The fibers, matrix and fillers are well bonded in the case of the composites fabricated with CuO than in those fabricated with TiO_2. The test composites fabricated with the CuO filler material show a higher glass transition temperature (22.22%) than that of the ones made with the TiO_2 filler. In the composites fabricated with CuO, greater interfacial adhesion and stress distribution among the fibers, matrices and the fillers were observed, and consequently they exhibited enhanced thermal characteristics, better than that of the composites produced with TiO_2. The surface morphology of the composites also supports these findings.

Acknowledgments

Institute of Radiation and Polymer Technology (IRPT), Atomic Energy Research Establishment, Savar, Dhaka; Institute of Energy Engineering, Dhaka University of Engineering and Technology (DUET), Gazipur, Dhaka; Bangladesh Ordnance Factories (BOF), Gazipur, Dhaka.

REFERENCES

[1] Meng F., Zheng S., Liu T., Epoxy resin containing poly(ethylene oxide)-block-poly(ε-caprolactone) diblock copolymer: effect of curing agents on nanostructures, Polymer 2006, 47(21), 7590-7600.

[2] Zhang D., Jia D., Toughness and strength improvement of diglycidyl ether of bisphenol-A by low viscosity liquid hyperbranched epoxy resin, J. Appl. Polym. Sci. 2006, 101(4), 2504-2511.

[3] Cabanelas J.C., Serrano B., Baselga J., Development of cocontinuous morphologies in initially heterogeneous thermosets blended with poly (methyl methacrylate), Macromolecules 2005, 38(3), 961-970.

[4] Francis B., Thomas S., Jose J., Ramaswamy R., Rao V.L., Hydroxyl terminated poly(ether ether ketone) with pendent methyl group toughened epoxy resin: miscibility, morphology and mechanical properties, Polymer 2005, 46(26), 12372-12385.

[5] Pickering S.J., Recycling technologies for thermoset composite materials – current status, Composite A 2006, 37(8), 1206-1215.

[6] Kim D.O., Keum S.W., Lee J.H., Lee J.H., Nam J.-D., Thermally expandable elastomer molding process for thermoset composite materials, Composite A 2006, 37(11), 2121-2127.

[7] Boyard N., Serre C., Vayer M., A physical approach to define a class A surface in polymer thermosetting composite materials, J. Appl. Polym. Sci. 2007, 103(1), 451-461.

[8] May C.A., Tanaka G.Y., Epoxy Resin Chemistry and Technology, Marcel Dekker, New York 1973.

[9] Baur R.S., Epoxy Resin Chemistry, Advances in Chemistry, vol. 114, American Chemical Society, Washington (DC) 1979.

[10] Potter W.G., Epoxide Resins, Springer, New York 1970.

[11] Maloth B., Srinivasulu N.V., Rajendra R., Influence of titanium oxide fillers on the tensile and flexural properties of E-glass fabric/epoxy composites, Materials Today: Proceedings 2020, 23 January.

[12] Hough J.A., Karad S.K., Jones F.R., The effect of thermal spiking on moisture absorption, mechanical and viscoelastic properties of carbon fibre reinforced epoxy laminates, Compos. Sci. Technol. 2005, 65(7-8), 1299-1305.

[13] Pereira A.B., de Morais A.B., Marques A.T., de Castro P.T., Mode II interlaminar fracture of carbon/epoxy multidirectional laminates, Compos. Sci. Technol. 2004, 64(10-11), 1653-1659.

[14] Kchaou A., Turki C., Salvia M., Fakhfakh Z., Tréheux D., Role of fibre–matrix interface and fibre direction on dielectric behaviour of epoxy composites, Compos. Sci. Technol. 2004, 64(10-11), 1467-1475.

[15] Tercjak A., Serrano E., Remiro P.M., Mondragon I., Viscoelastic behavior of thermosetting epoxy mixtures modified with syndiotactic polystyrene during network formation, J. Appl. Polym. Sci. 2006, 100(3), 2348-2355.

[16] Salmon N., Carlier V., Schut J., Remiro P.M., Mondragon I., Curing behaviour of syndiotactic polystyrene-epoxy blends, 1. Kinetics of curing and phase separation process, Polym. Int. 2005, 54(4), 667-672.

[17] Francis B., Ramaswamy R., Rao V.L., Jose S., Thomas S., Raju K.V.S.N., Morphology, viscoelastic properties, and mechanical behavior of epoxy resin modified with hydroxyl-terminated poly(ether ether ketone) oligomer with pendent tert-butyl groups, Polym. Eng. Sci. 2005, 45(12), 1645-1654.

[18] Ferreira J.M., Errajhi O.A.Z., Richardson M.O.W., Thermogravimetric analysis of aluminized E-glass fiber reinforced unsaturated polyester composites, Polymer Test. 2006, 25, 1091-1094.

[19] Hammed N., Sreekumar P.A., Francis B. et al., Morphology, dynamic mechanical and thermal studies on poly (styrene-Co-acrylonitrile) modified epoxy resin/glass fibre composites, Composites Part A: Appl. Sci. Manuf. 2007, 38, 2422--2432.

[20] Yusri H.M., Sahrim A., Mechanical and thermal properties of glass fiber-reinforced epoxy composite with matrix modification using liquid epoxidized natural rubber, J. Reinfor. Plast. Compos. 2013, 32(9), 612-618.

[21] Deep N., Mishra P., Evaluation of mechanical properties of functionalized carbon nanotube reinforced PMMA polymer nanocomposite, Karbala Int. J. Modern Sci. 2018, 4, 207--215.

[22] Yang H.H., [In:] Bunsell A.R., editor, Fiber Reinforcement of Composite Materials, Elsevier, Amsterdam 1988, 246--329.

[23] Young R.J., Lu D., Day R.J., Knoff W.F., Davis H.A., Relationship between structure and mechanical properties for aramid fibers, J. Mater. Sci. 1992, 27, 5431-5440, DOI: 10.1007/BF00541602.

[24] Chinnasamy V., Subramani S.P., Palaniappan S.K., Mylsamy B., Aruchamy K., Characterization on thermal properties of glass fiber and kevlar fiber with modified epoxy hybrid composites, J. Mater. Res. Technol. 2020, 9(3), 3158--3167, DOI: 10.1016/j.jmrt.2020.01.061.

